

## Orientation Features of $^{24}\text{Mg}(2^+)$ Aligned Nuclei in $(p,p)$ and $(d,d)$ Reactions at $E_x \approx 7.5$ MeV per Nucleon

L. I. Galanina\*, N. S. Zelenskaya, V. M. Lebedev, N. V. Orlova, and A. V. Spassky

*Skobeltsyn Institute of Nuclear Physics, Moscow State University, Moscow, 119991 Russia*

Received January 19, 2015

**Abstract**—Experimental angular dependences of cross sections for elastic and inelastic scattering and the result obtained by reconstructing the populations of magnetic sublevels, multipole-moment orientation tensors, and polarization tensors are presented for  $^{24}\text{Mg}(2^+, 1.369 \text{ MeV})$  aligned nuclei produced in inelastic proton scattering at  $E_p = 7.4 \text{ MeV}$ . The experimental results in question are compared with the results of calculations based on the coupled-channel method and on the compound-nucleus model, the  $3/2^+$  resonance in the  $^{25}\text{Al}$  compound nucleus being taken into account. The orientation features of  $^{24}\text{Mg}(2^+, 1.369 \text{ MeV})$  nuclei produced in inelastic proton and deuteron scattering on  $^{24}\text{Mg}$  at  $E_x \approx 7.5 \text{ MeV}$  per nucleon are found to be generally similar despite a substantial difference in the respective differential cross sections.

**DOI:** 10.1134/S1063778815060095

### 1. INTRODUCTION

Investigation of angular correlations of products of nuclear reactions that belong to the  $A(x,y)B^*(J_B)$  type and in which one detects, in several planes with respect to the reaction plane, gamma rays removing the excitation of nucleus  $B^*$  is one of efficient methods for studying the structure of excited oriented nuclei and reaction mechanisms [1]. Such experiments make it possible to reconstruct the spin-tensor components of the density matrix for the  $B^*(J_B)$  excited nucleus and, on this basis, to find its other correlation features.

In [2–5], our group presented the results of  $\alpha\gamma$  and  $d\gamma$  correlation experiments devoted to studying inelastic alpha-particle ( $E_\alpha = 30.3 \text{ MeV}$ ) and deuteron ( $E_d = 15.3 \text{ MeV}$ ) scattering leading to the formation of a  $^{24}\text{Mg}$  final nucleus in the  $2^+$  state at 1.369 MeV. We showed that, in order to describe qualitatively the  $\alpha\gamma$  correlation features found in this way, it is sufficient to employ a collective mechanism within the coupled-channel method on the basis of a simple rotational model and the same mechanism with allowance for spin-orbit and tensor interactions in order to describe correctly deuteron scattering. The present article reports on a continuation of particle-gamma ray correlation experiments that study the production of  $^{24}\text{Mg}$  aligned nuclei.

A priori, it is clear that, in proton scattering on  $^{24}\text{Mg}$  nuclei, the effect of tensor forces should not

be substantial; at the same time, it follows from the analysis in [6] that the inclusion of a resonance excitation of individual levels of  $^{25}\text{Al}$  within the compound-nucleus model may be of importance. In the study of our group reported in [7], we showed that, upon combining the assumption that a  $3/2^+$  resonance exists in the  $^{25}\text{Al}$  compound nucleus at 9.4 MeV with a collective excitation mechanism within the coupled-channel method, one can match cross sections for elastic and inelastic proton scattering with respective experimental data and obtain a qualitative description of the experimental  $p\gamma$  angular-correlation function and spin-tensor components of the density matrix.

The experimental procedure used permits both obtaining ordinary angular distributions of differential cross sections and reconstructing the angular dependences of all nine even-even spin-tensor components of the density matrix for the  $^{24}\text{Mg}$  nucleus in the  $2^+$  state at 1.369 MeV. This made it possible to determine a complete set of orientation features of the aligned nucleus being studied—namely, the population of magnetic substates; the tensors of orientation of its multipole moments; and the tensor polarization—both quadrupole and hexadecapole. Similar theoretical quantities were calculated by the coupled-channel method [8] (with the aid of the CHUCK [9] and FRESCO [10] codes) and on the basis of the compound-nucleus model under the assumption that a  $3/2^+$  resonance is formed in the  $^{25}\text{Al}$  nucleus. The results (both experimental and theoretical) were compared with their counterparts

\*E-mail: wg2@anna19.sinp.msu.ru

for inelastic deuteron scattering at  $E_d = 15.3$  MeV on  $^{24}\text{Mg}$  that goes over to the same  $2^+$  state at 1.369 MeV. Despite a significant difference of the  $(p, p')$  and  $(d, d')$  differential cross sections, the experimental orientation features of  $^{24}\text{Mg}$  aligned nuclei produced in the  $2^+$  state at 1.369 MeV upon inelastic proton and deuteron scattering are in general qualitatively similar.

## 2. EXPERIMENTAL PROCEDURE

Our experiment was performed at the U-120 cyclotron of the Institute of Nuclear Physics (Moscow State University) by using protons accelerated to an energy of 7.4 MeV, the energy spread of the beam being about 70 keV. A self-supporting magnesium film  $0.77 \text{ mg cm}^{-2}$  thick enriched to 97% in the isotope  $^{24}\text{Mg}$  was used as a target. The error in the absolute values of the differential cross section was about 20% and was determined primarily by the uncertainties in the measurement of the target thickness and in the calibration of the beam-current integrator.

Up to four surface-barrier silicon semiconductor detectors characterized by a sensitive-region thickness of up to  $350 \mu\text{m}$  were used to detect protons. The detectors were arranged within the scattering chamber 23 cm in diameter on a movable arc whose rotation angle with respect to the horizontal plane could be changed from 0 to  $90^\circ$ . In measuring double-differential cross sections, the angular resolution of the semiconductor detectors was  $\pm 2^\circ$ .

Gamma rays were detected in the range of the emission angle  $\theta_\gamma$  between  $20^\circ$  and  $150^\circ$  by four BDEG-23 scintillation detectors based on NaI(Tl) crystals 63 mm in height and in diameter. These detectors were mounted at a fixed angular interval of  $\Delta\theta_\gamma = 32.5^\circ$  on a movable horizontal ring platform outside the scattering chamber. The angular resolution of the gamma detectors was  $\pm 13^\circ$ , and we took into account corrections for it in analyzing experimental data. The relative efficiency of the gamma detectors was tested by rotating the platform through an angle of  $32.5^\circ$ , whereby a repeated measurement (at three values of the angle  $\theta_\gamma$ ) of the double-differential cross section with alternating gamma detectors was ensured. The detection of  $p\gamma$  coincidences was performed at gamma-ray energies between 0.6 and 1.5 MeV. A detailed description of the experimental equipment used and of the respective measuring and computational complex can be found in [11]. The double-differential cross section  $W(\theta_\gamma, \varphi_\gamma; \theta_p)$  for the reaction  $^{24}\text{Mg}(p, p\gamma_{1.369})^{24}\text{Mg}$  was measured for 16 values of the laboratory proton scattering angle  $\theta_p$  from  $30^\circ$  to  $160^\circ$  in three photon-detection planes of  $\varphi_\gamma = 180^\circ, 225^\circ, \text{ and } 270^\circ$ . The

average value of the respective statistical error was about 14%.

The angular dependence of the differential cross section was measured in a dedicated experiment with the aid of a semiconductor detector positioned outside the scattering chamber and characterized by the angular resolution of  $\pm 1^\circ$ . In that case, protons originating from the reaction being studied were extracted from the chamber through a horizontal slit closed by a thin Mylar window. The error in determining zero angle was within  $\pm 1^\circ$ . The statistical uncertainty in the differential cross section did not exceed 5%.

For each value of  $\theta_p$ , the double-differential cross section  $W(\theta_\gamma, \varphi_\gamma; \theta_p) = d^2\sigma/d\Omega_\gamma d\Omega_p$  was parametrized in the form [1]

$$W(\theta_\gamma, \varphi_\gamma; \theta_p) = \frac{1}{\sqrt{4\pi}} \sum_{k\kappa} \frac{1 + (-1)^k}{\sqrt{2k+1}} \quad (1) \\ \times A_{k\kappa}(\theta_p) Y_{k\kappa}^*(\theta_\gamma, \phi_\gamma),$$

where  $Y_{k\kappa}^*(\theta_\gamma, \varphi_\gamma)$  are conjugate spherical harmonics depending on the photon emission angles  $\theta_\gamma$  and  $\varphi_\gamma$  in the system of spherical coordinates whose  $Z$  goes along the projectile momentum and whose  $(X, Z)$  plane coincides with the reaction plane (in the “experimental” coordinate frame) and  $A_{k\kappa}(\theta_p)$  are real-valued parameters that coincide, apart from factors, with the spin-tensor components  $\rho_{k\kappa}(\theta_p)$  of the density matrix for the final-state nucleus. Summation in expression (1) is performed over even values of the rank  $k$  of spin-tensor components ( $k = 0, 2, \text{ and } 4$ ) and over all possible projections  $\kappa$  from  $-k$  to  $k$ . Since  $^{24}\text{Mg}$  in the  $2^+$  state goes over to the ground state via an  $E2$  transition, our experiment makes it possible to reconstruct all nine even components  $A_{k\kappa}(\theta_p)$ . The values found for  $A_{k\kappa}(\theta_p)$  were then used to determine the orientation features of the final-state nucleus. For each value of the angle  $\theta_p$ , the absolute values of the double-differential cross section were obtained from the condition  $A_{00}(\theta_p) = \rho_{00}(\theta_p) \equiv d\sigma/d\Omega(\theta_p)$ .

## 3. ORIENTATION FEATURES RECONSTRUCTED FOR $^{24}\text{Mg}$ ALIGNED NUCLEI IN THE $2^+$ STATE FROM SPIN-TENSOR COMPONENTS OF THE DENSITY MATRIX

Knowledge of the spin-tensor components  $\rho_{k\kappa}(\theta_p)$  of the density matrix makes it possible to determine basic orientation features of Mg nuclei in the  $2^+$  state—namely, the populations  $P_{\pm M}(J_B, \theta_p)$  of magnetic substates of the spin  $J_B$ , the multipole-moment orientation tensors  $t_{k\kappa}(\theta_y)$ , and the polarization tensors  $T_{k\kappa}(\theta_y)$ . Below, we present formulas that permit

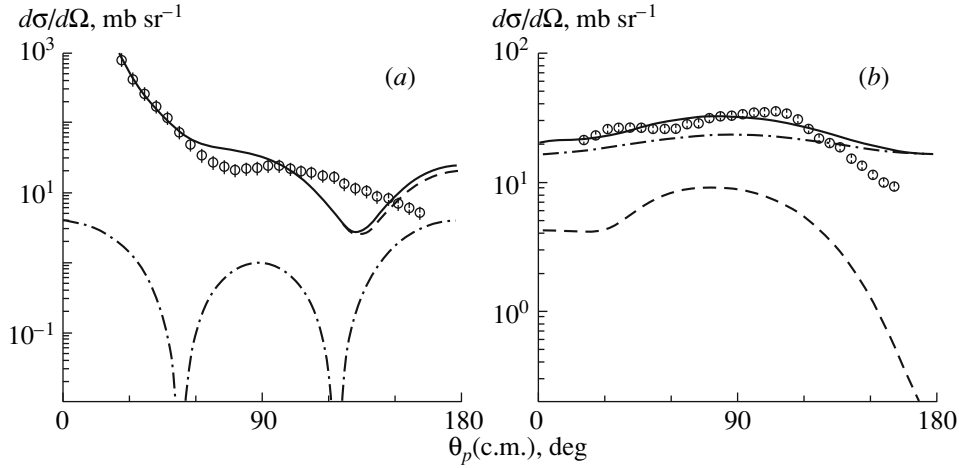


**Fig. 1.** Experimental angular dependences (open circles) of the differential cross sections for (a) elastic and (b) inelastic proton scattering on  $^{24}\text{Mg}$  nuclei at  $E = 7.4$  MeV along with the results of theoretical calculations. The statistical errors that exceed the point size are indicated in this figure and in the figures that follow. The displayed theoretical curves represent (dashed curve) the results of the calculations based on the coupled-channel method, (dash-dotted curve) the contribution of the  $J(^{25}\text{Al}) = 3/2^+$  resonance, and (solid curve) the total contribution of these two mechanisms.

calculating the above features in terms of the spin-tensor components  $\rho_{k\kappa}(\theta_p)$ .

The populations  $P_{\pm M}(J_B, \theta_p)$  are determined by the ratio of the diagonal elements of the density matrix to its trace [which coincides with  $\rho_{00}(\theta_y)$ ] in the coordinate frame where the  $z$  axis coincides in direction with the spin of the nucleus and is orthogonal to the reaction plane. A transition to this reference frame from the “experimental” one is accomplished with the aid of the Wigner function  $D_{\kappa 0}^k(\pi/2, \pi/2, \pi/2)$  as

$$\begin{aligned} \rho_J(M, M) &= \frac{1}{\sqrt{(2J+1)}} \frac{1}{\rho_{00}(\theta_y)} \\ &\times \sum_{k\kappa} (-1)^{J-M} \langle JM J - M | k0 \rangle \\ &\times \rho_{k\kappa}(\theta_y) D_{\kappa 0}^k(\pi/2, \pi/2, \pi/2). \end{aligned} \quad (2)$$

The multipole-moment orientation tensors  $t_{k\kappa}(\theta_y)$  are determined in the coordinate frame where the  $z$  axis is aligned with the recoil-nucleus momentum; that is,

$$t_{k\kappa}(\theta_y) = \frac{1}{\sqrt{(2k+1)(2J_B+1)}} \frac{\rho_{k\kappa}(\theta_y)}{\rho_{00}(\theta_y)}. \quad (3)$$

A transition to this coordinate frame from the “experimental” one is performed by means of the Wigner function  $D(\pi, \pi - \theta_y, \pi)$ . The orientation tensors  $t_{k\kappa}(\theta_y)$  relate the matrix element of the respective multipole-moment operator with a rank satisfying the condition  $k \leq 2J_B$  to its reduced matrix element as

$$\langle J_B M | Q_{k\kappa} | J_B M \rangle = t_{k\kappa}(\theta_y) \langle J_B || Q_{k\kappa} || J_B \rangle. \quad (4)$$

The tensor polarization  $T_{k\kappa}(\theta_y)$  is determined in the coordinate frame whose  $z$  axis is orthogonal to the reaction plane and whose  $x$  axis is aligned with the incident-beam momentum. A transition to this coordinate frame from that in which the quantities  $\rho_{k\kappa}(\theta_y)$  were reconstructed on the basis of experimental data is accomplished by means of three successive rotations through the Euler angles  $\alpha = \pi/2$ ,  $\beta = \pi/2$ , and  $\gamma = \pi$ . As a result, the tensor polarization is expressed in terms of the reconstructed spin-tensor components of the density matrix for the nucleus under study as [12–14]

$$\begin{aligned} T_{k\kappa}(\theta_y) &= \frac{1}{\sqrt{(2J+1)}} \sum_{\pm\kappa'} \frac{\rho_{k\kappa'}(\theta_y)}{\rho_{00}(\theta_y)} \\ &\times D_{\kappa'\kappa}^k(\pi/2, \pi/2, \pi). \end{aligned} \quad (5)$$

#### 4. RESULTS OF OUR MEASUREMENTS

The angular dependences of the differential cross sections for elastic proton and deuteron scattering on  $^{24}\text{Mg}$  nuclei and the respective inelastic-scattering processes leading to the transition of these nuclei to the  $2^+$  state of  $^{24}\text{Mg}$  at 1.369 MeV are shown in Figs. 1 and 2. By employing the experimental spin-tensor components of the density matrix from [2, 7], we found the populations  $P_{\pm M}(\theta_y)$  for all projections  $M = 0, 1$ , and 2 of the  $^{24}\text{Mg}(2^+)$  spin of  $J_f = 2$  with the aid of Eq. (2). The results are given in Fig. 3. Equations (3) and (5) were used to reconstruct experimental angular dependences of polarization features of the  $^{24}\text{Mg}(2^+)$  nucleus for inelastic proton scattering. The respective results are shown in Fig. 4 for

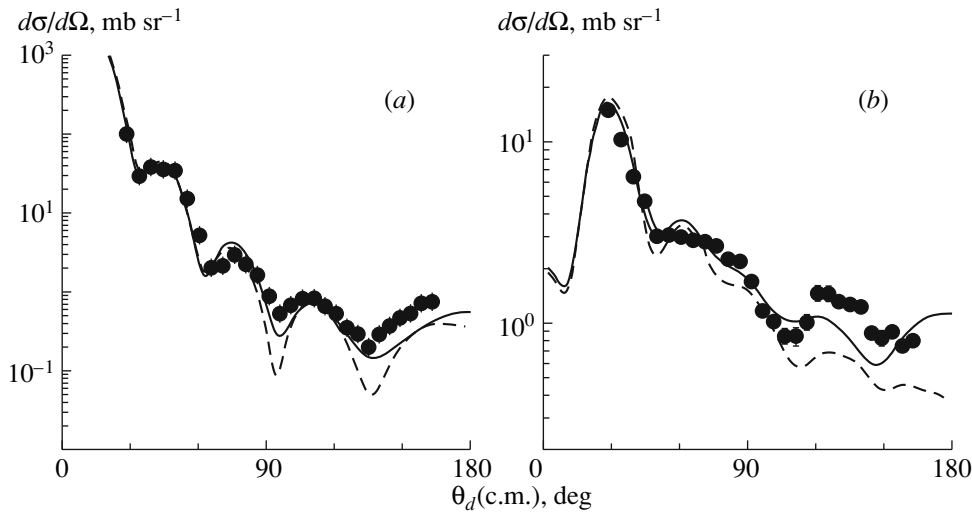


**Fig. 2.** As in Fig. 1 (the closed circles represent experimental data), but for deuteron scattering on  $^{24}\text{Mg}$  at  $E_d = 15.3$  MeV, along with the results of theoretical calculations. The solid and dashed curves were calculated on the basis of the coupled-channel method (FRESCO code), respectively, with and without allowance tensor forces.

the components of the multipole-moment orientation tensors  $t_{k\kappa}(\theta_p)$  and in Fig. 5 for the components of the polarization tensors.

## 5. ANALYSIS OF OUR RESULTS

In the present study, we consider two mechanisms of inelastic proton scattering at an energy of 7.4 MeV—that is, a collective interaction within the coupled-channel method and the compound-nucleus model. A significant contribution of this collective interaction is due primarily to a large static quadrupole deformation of the  $^{24}\text{Mg}$  nucleus.

The compound-nucleus model is considered upon taking into account individual isolated resonances or upon going over to statistical limit of strongly overlapped resonances. For inelastic proton scattering, the excitation energy of the  $^{25}\text{Al}$  compound nucleus is about 9.4 MeV, exceeding the energies of known levels from nuclear databases [15]. The results obtained

by analyzing the energy dependences of the cross sections for elastic and inelastic proton scattering on  $^{24}\text{Mg}$  in the vicinity of the above energy value suggest the presence of individual resonance levels of the  $^{25}\text{Al}$  compound nucleus [16]—in particular, a  $3/2^+$  resonance. In view of the foregoing, we analyzed the experimental features in question on the basis of the compound-nucleus model, assuming the formation of a  $3/2^+$  isolated resonance in the  $^{25}\text{Al}$  nucleus.

In the rotational model of the nucleus, the coupled-channel method was applied within the ground-state rotational band ( $0^+ \rightarrow 2^+ \rightarrow 4^+$ ). The calculations based on this model were performed with the aid of the CHUCK [9] and FRESCO [10] codes. The spin-tensor components of the resonance-process density matrix for  $A(x, y)B$  reactions were calculated by the formula [17]

$$\begin{aligned} \rho_{k\kappa}(\theta_y) = & \frac{1}{2\pi^2 k_x^2} \frac{k_y}{k_x} \frac{\sqrt{2J_B + 1}}{(2J_A + 1)(2J_x + 1)} \sum_{\lambda\lambda'} \left[ (E - E_\lambda)^2 + \frac{1}{4} \Gamma_\lambda \Gamma'_\lambda \right]^{-1} (2J_c + 1)^2 \\ & \times \sum (-1)^{S_f - S'_f + l + l' - m'_l} \sqrt{(2S_f + 1)(2S'_f + 1)(2l + 1)(2l' + 1)(2L_x + 1)(2L'_x + 1)} \\ & \times \langle L_x 0 L_y m_l | l m_l \rangle \langle L'_x 0 L'_y m'_l | l' m'_l \rangle \langle l m_l l' m'_l | k \kappa \rangle \\ & \times W(S_i L_x S_f L_y : J_c l) W(S_i L'_x S'_f L'_y : J_c l') W(J_B S_f J_B S'_f : J_y k) \\ & \times W(l S_f l' S'_f : S_i k) \left| \gamma_{L_x S_i}^\lambda \gamma_{L_y S_f}^\lambda \cdot I_{L_x S_i}^{J_c} \cdot I_{L_y S_f}^{J_c} \right|^2 \bar{P}_{L'_y m'_l}^*(\theta_y) \bar{P}_{L_y m_l}(\theta_y). \end{aligned} \quad (6)$$

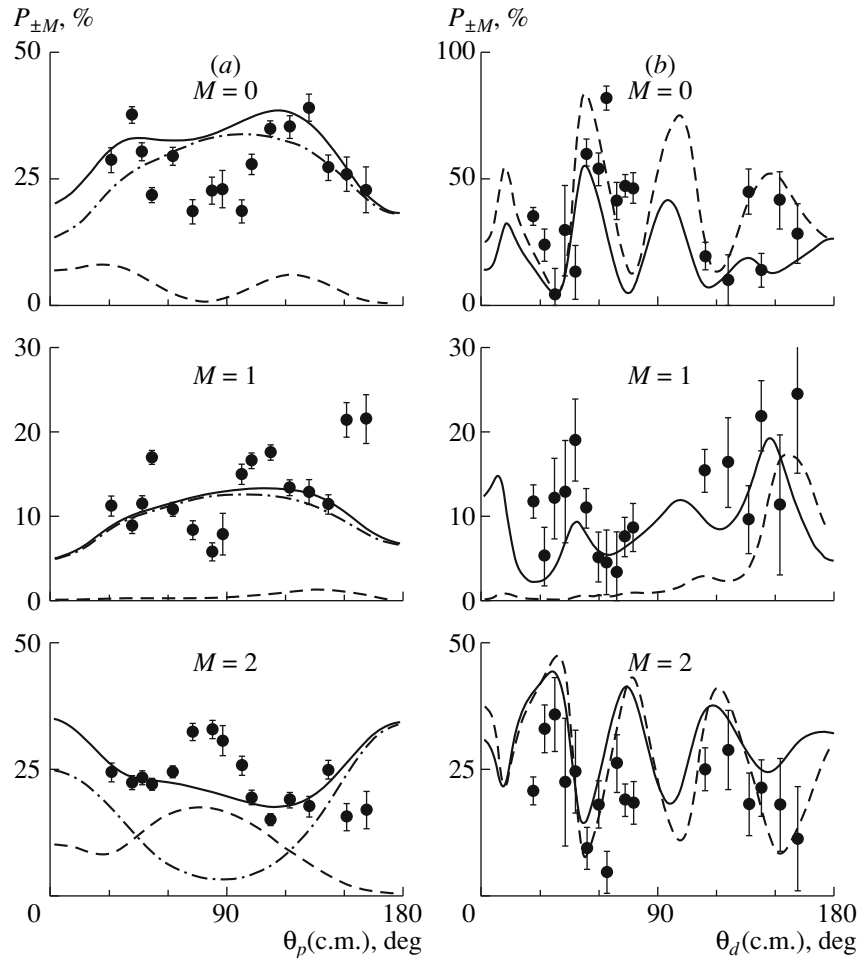


**Fig. 3.** Angular dependences of the populations of magnetic sublevels of the  $^{24}\text{Mg}$  nucleus in the  $2^+$  state at 1.369 MeV formed upon inelastic (a) proton and (b) deuteron scattering at an energy of  $E \approx 7.5$  MeV per nucleon for various values of the spin projection  $M$ . The closed circles represent experimental data. The notation for the curves in Figs. 3a and 3b is identical to that in Figs. 1 and 2, respectively.

In expression (6),  $E_i$  ( $E_f$ ) is the c.m. kinetic energy of particle  $x$  ( $y$ );  $J_c$  is the total spin of the compound-nucleus level;  $S_i$  ( $S_f$ ) is the spin of the initial (final) channel;  $L_x$  ( $L_y$ ) is the orbital angular momentum of distorted partial waves in the entrance (exit) reaction channel; and  $|\gamma_{L_x S_i}^{J_c}|^2$  ( $|\gamma_{L_y S_f}^{J_c}|^2$ ) is the partial width with respect to the decay of the compound-nucleus resonance with spin  $J_c$  in the entrance (exit) channel, the amplitudes of these widths being related to the reduced resonance-decay widths by the equations [18]

$$\gamma_{L_x S_i}^{J_c} = \left( \frac{\hbar^2}{\mu_x A R^2} \right)^{1/2} \theta_{L_x S_i J_c}^{C \rightarrow x+A},$$

$$\gamma_{L_y S_f}^{J_c} = \left( \frac{\hbar^2}{\mu_x A R^2} \right)^{1/2} \theta_{L_y S_f J_c}^{C \rightarrow y+B},$$

where  $R$  is the radius of nucleus  $C$ . The quantity  $\Gamma_\lambda$  is the total width of the resonance level characterized by an energy  $E_\lambda$  and a spin  $J_c$ ; that is,

$$\Gamma_\lambda = \sum_{S_i L_x} \left| \gamma_{L_x S_i}^{J_c=\lambda} \right|^2. \quad (7)$$

The differential reaction cross section is determined by the spin-tensor component of zero rank. After a transformation of the product of associated Legendre polynomials in expression (6) and summation of respective Clebsch–Gordan and Racah coefficients, we can recast the differential cross section for resonance excitation into the form [19]

$$\frac{d\sigma}{d\Omega}(\theta_y) = \frac{1}{4\pi^2} \frac{1}{k_x^2} \frac{k_y}{k_x} \frac{1}{(2J_A + 1)(2J_x + 1)} \quad (8)$$

$$\times \sum_{S_i S_f L} (-1)^{S_i - S_f} \left[ (E - E_L)^2 + \frac{1}{4} \Gamma_L^2 \right]^{-1}$$

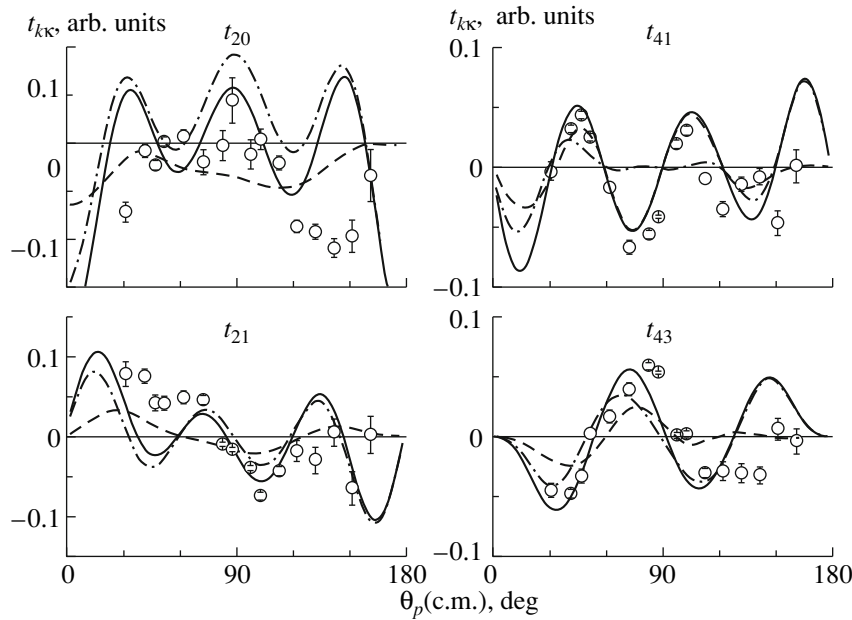


**Fig. 4.** Angular dependences of components of the multipole-moment quadrupole and hexadecapole orientation tensors for  $^{24}\text{Mg}$  nuclei formed in the  $2^+$  state at 1.369 MeV upon inelastic proton scattering at  $E_p = 7.4$  MeV. The open circles represent experimental data. The notation for the curves is identical to that in Fig. 1.

$$\begin{aligned} & \times (2J_c + 1)^2 \sum_{L_x L'_x L_y L'_y} W(L_x J L'_x J : S_i L) \\ & \times W(L_y J L'_y J : S_f L) \left| \gamma_{L_x S_i}^\lambda \gamma_{L_y S_f}^\lambda \cdot I_{L_x S_i}^{J_c} \cdot I_{L_y S_f}^{J_c} \right|^2 \\ & \times \sum \sqrt{(2L_x + 1)(2L'_x + 1)(2L_y + 1)(2L'_y + 1)} \\ & \times \langle L_x 0 L'_x 0 | L 0 \rangle \langle L_y 0 L'_y 0 | L 0 \rangle P_L(\theta_y). \end{aligned}$$

In order to calculate distorted waves in the entrance and exit channels, the global optical potential (OP) proposed in [20], which includes spin-orbit interaction and which describes fairly well the angular distribution for the elastic channel in the forward region of proton emission angles at an energy of 7.4 MeV, was chosen as an optical potential of  $p^{24}\text{Mg}$  interaction both for the collective mechanism in the coupled-channel method and for the mechanism of resonance excitation in a compound nucleus. The parameters of this potential were not varied in our calculations.

For the mechanisms used, the total angular distribution of the differential cross section for inelastic scattering was determined as the sum of the calculated cross sections for the collective and resonance processes, the relative contribution of the latter being found from an optimum fit of the sum of the differential cross sections to the experimental angular distribution.

In Fig. 1, the experimental angular distributions for elastic proton scattering on  $^{24}\text{Mg}$  nuclei to their ground state and for the respective inelastic process leading to the transition of these nuclei to the first excited state at 1.369 MeV, whose spin-parity is  $2^+$ , are contrasted against the results of respective calculations.

This figure shows that, for elastic proton scattering (Fig. 1a), the collective-excitation mechanism calculated by the coupled-channel method provides a satisfactory description of the differential cross section in the forward hemisphere of proton emission angles, but, in the region of large angles, the theoretical cross sections deviate from experimental data even qualitatively. As the angle becomes larger, the experimental cross section decreases smoothly, while the cross section calculated by the coupled-channel method has a minimum at  $\theta_p \approx 130^\circ$  and exhibits a sizable growth at large angles. For elastic proton scattering, the contribution of the mechanism involving the excitation of the  $3/2^+$  resonance in  $^{25}\text{Al}$  proved to be insignificant.

In the case of inelastic proton scattering (see Fig. 1b), the contributions of the different mechanisms change drastically. The collective-excitation mechanism yields a differential cross section for protons that differs from the experimental cross section nearly by one order of magnitude. The inclusion of the  $3/2^+$  resonance leads to an increase in the differential

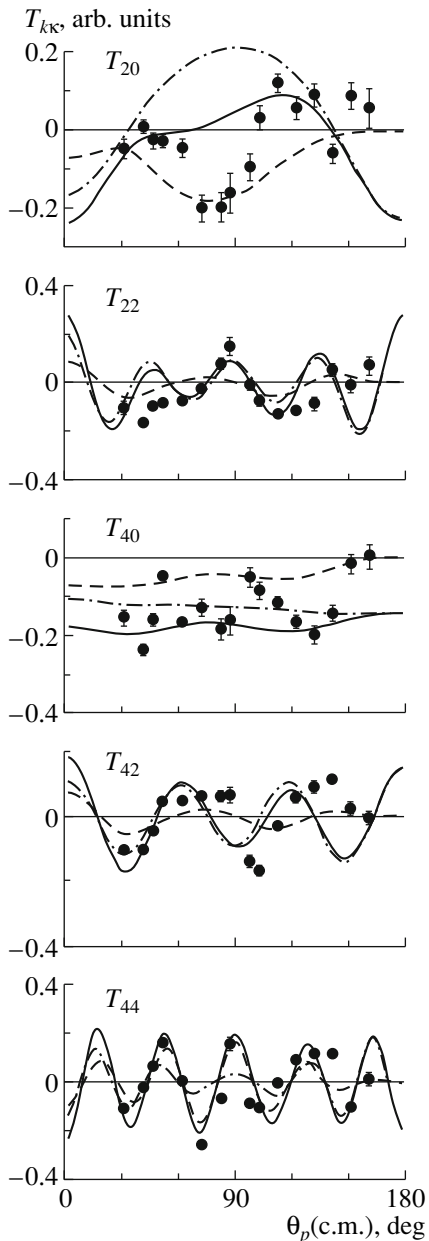


**Fig. 5.** Angular dependences of components of the tensor polarization  $T_{k\kappa}(\theta_p)$  of  $^{24}\text{Mg}$  nuclei formed in the  $2^+$  state upon inelastic scattering protons at  $E_p = 7.4$  MeV. The closed circles represent experimental data. The notation for the curves is identical to that in Fig. 1.

cross section as a function of the scattering angle. Only at large proton-emission angles does the theoretical differential cross section for inelastic proton scattering deviate from experimental data.

Figure 2 illustrates a comparison of experimental angular distributions for deuteron scattering leading to the formation of the same states of  $^{24}\text{Mg}$  with the results of the calculations based on the coupled-channel method. The solid (dashed) curves repre-

sent the cross sections calculated according to the FRESKO code by using the global  $d^{24}\text{Mg}$  potential from [20] with (without) allowance for tensor forces. From this figure, one can see that, within the rotational model, the coupled-channel method implemented with allowance for a noncentral tensor interaction yields cross sections that agree with their experimental counterparts up to an angle of  $\theta_d \sim 100^\circ$ . At angles larger than  $100^\circ$ , the experimental cross sections somewhat exceed the calculated cross sections.

Thus, it is important to take into account, in addition to the collective mechanism, the excitation of the  $3/2^+$  resonance in a  $^{25}\text{Al}$  compound nucleus in order to describe experimental angular distributions for proton scattering on  $^{24}\text{Mg}$  nuclei and a noncentral tensor interaction within the coupled-channel method in order to reach this goal for deuteron scattering.

We will now compare the calculated and experimental features of inelastic proton and deuteron scattering on  $^{24}\text{Mg}$  nuclei. Figure 3a shows the experimental and calculated (with allowance for both mechanisms) angular dependences of the populations  $P_{\pm M}(\theta_p)$  for  $^{24}\text{Mg}$  in the case of proton scattering. The calculation reproduces qualitatively the experimental dependences of  $P_{\pm M}(\theta_p)$  on the proton emission angle. The discrepancy between the experimental and theoretical values of  $P_{\pm M}(\theta_p)$  reaches the greatest values at angles around  $\theta_p \sim 90^\circ$ —that is, in a region where the differential cross section calculated for inelastic proton scattering agrees fairly well with experimental data. It is noteworthy that the contribution of the collective mechanism is of importance in describing the population  $P_{\pm 2}(\theta_p)$ .

A comparison of the experimental and calculated angular dependences of the populations  $P_{\pm M}(\theta_d)$  for deuteron scattering is illustrated in Fig. 3b. In the calculation of the populations in question, the inclusion of spin-orbit and tensor interactions proved to be of crucial importance. Without the inclusion of these interactions, the theoretical values of  $P_{\pm 1}(\theta_d)$  are zero. Only upon taking into account a tensor interaction does a maximum commensurate in amplitude with the experimental maximum appear in the region of small angles in the angular dependence of  $P_{\pm 1}(\theta_d)$ . It is noteworthy that a variation of the parameters in the tensor component of the potential causes the greatest change in the population of substates of the  $|M| = 1$  level at large angles, and this is an angular region where the calculated curve for  $P_{\pm 1}(\theta_d)$  shows the smallest deviation from the respective experimental dependence.

Figures 4 and 5 illustrate a comparison of the experimental and theoretical angular dependences

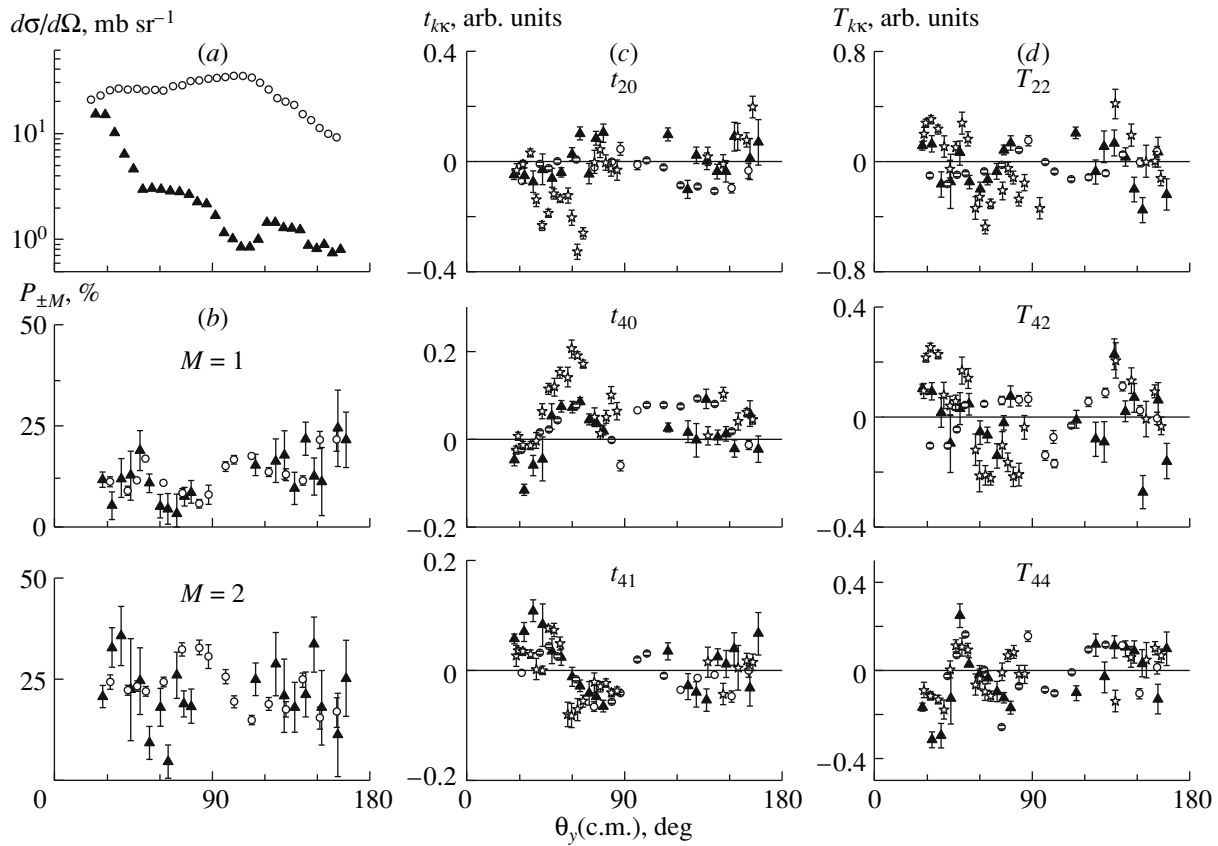


**Fig. 6.** (a) Differential cross sections, (b) populations of magnetic substates, (c) several experimental components of multipole-moment orientation tensors, and (d) tensor polarization for  $^{24}\text{Mg}$  nuclei formed in the  $2^+$  state upon inelastic (open circles) proton, (closed triangles) deuteron, and (stars) alpha-particle scattering at an energy of  $E \approx 7.5$  MeV per nucleon.

of polarization features of  $^{24}\text{Mg}$  nuclei formed in the  $2^+$  state upon proton scattering. The theoretical multipole-moment orientation tensors  $t_{k\kappa}(\theta_p)$  for  $k = 2$  and  $4$  (see Fig. 4) that were calculated with allowance for the aforementioned mechanisms correctly reproduce an oscillating character of their experimental counterparts, but, in the region of large angles, the deviation from experimental data is sizable. A collective mechanism that takes into account the static deformation of  $^{24}\text{Mg}$  nuclei ( $\beta_2 = 0.4$ ) makes a significant contribution to nearly all of the components of  $t_{k\kappa}(\theta_p)$ , especially at small values of the angle  $\theta_p$ . A similar picture is observed for the  $k = 2$  and  $4$  components of the tensor polarization  $T_{k\kappa}(\theta_y)$  (see Fig. 5).

In Fig. 6, the experimental orientation features of inelastic proton, deuteron, and alpha-particle scattering on  $^{24}\text{Mg}$  nuclei are presented at the same energy per nucleon. This figure shows that, despite a drastically different behavior of the angular distributions of differential cross sections (see Fig. 6a) in the respective ( $p, p'$ ) and ( $d, d'$ ) reactions, the reconstructed

populations (see Fig. 6b) agree reasonably well, especially for the spin-projection value of  $M = 1$ . A similar picture is also observed for the majority of the components of  $t_{k\kappa}(\theta_y)$  (Fig. 6c) and  $T_{k\kappa}(\theta_y)$  (Fig. 6d) for all cases, including the case of  $^{24}\text{Mg}$  production in the  $2^+$  state upon inelastic alpha-particle scattering. The similarity of  $T_{k\kappa}(\theta_y)$  for  $^{24}\text{Mg}$  nuclei produced in the  $2^+$  state upon inelastic deuteron and alpha-particle scattering was highlighted earlier in [3].

This effect may be due to the following reasons. First, all of the orientation features considered here are normalized by definition to the differential cross section for inelastic scattering, and this may level out the possible distinctions between the quantities in question to some extent.

Second, this may be due a feature characterizing the angular dependence of the tensors  $t_{k0}(\theta_y)$  [21] for inelastic scattering of light particles on even-even nuclei that leads to the excitation of the spin- $J_B$  state at moderately small values of  $\theta_y$ . Indeed, we can see that, for  $\theta_y \rightarrow 0^\circ$ , the spin projection onto the axis of the nucleus is  $M = M' = 0$ . According to the

definition of the  $\kappa = 0$  spin-tensor components of the density matrix [1], we have

$$\rho_{k0}(\theta_y \approx 0^\circ) = \sqrt{2J_B + 1} \quad (9)$$

$$\times (-1)^{J_B} \langle J_B 0 J_B 0 | k 0 \rangle |M_{if}(\theta_y \approx 0^\circ)|^2,$$

where  $M_{if}(\theta_y \approx 0^\circ)$  is reaction matrix element. According to the definition in (3), the orientation tensors  $t_{k0}(\theta_y \approx 0^\circ)$  then have the form

$$t_{k0}(\theta_y \approx 0^\circ) \quad (10)$$

$$= \frac{(-1)^{J_B} \langle J_B 0 J_B 0 | k 0 \rangle |M_{if}(\theta_y \approx 0^\circ)|^2}{\sqrt{2k+1} |M_{if}(\theta_y \approx 0^\circ)|^2},$$

or

$$t_{k0}(\theta_y = 0^\circ, \tilde{\theta}_y = \pi) = \frac{(-1)^{J_B} \langle J_B 0 J_B 0 | k 0 \rangle}{\sqrt{2k+1}}; \quad (11)$$

that is, the orientation tensors for the aligned nucleus in the  $2^+$  state at  $\theta_y = 0^\circ$  do not depend on the structure of the target nucleus or on the scattering mechanism. As a result, we have

$$t_{20}(\theta_y = 0^\circ) = -\sqrt{\frac{2}{35}} = -0.239, \quad (12)$$

$$t_{40}(\theta_y = 0^\circ) = \sqrt{\frac{2}{35}} = 0.239;$$

that is, both the quadrupole and the hexadecapole orientation tensor at  $\theta_y = 0^\circ$  are constants and coincide, apart from the sign. This circumstance may have a pronounced effect on the general behavior and similarity of orientation features at small scattering angles.

Finally, the contribution of the collective scattering mechanism associated with a large static deformation of the  $^{24}\text{Mg}$  nucleus may also be one of the reasons behind the similarity of orientation features in the reactions considered here.

## 6. CONCLUSIONS

From the analysis of the angular dependences of correlation features that was performed by our group in [3, 4] for  $^{24}\text{Mg}$  nuclei produced in the  $2^+$  state upon inelastic deuteron and alpha-particle scattering, it was found that a dominant mechanism of the respective ( $d, d'$ ) and ( $\alpha, \alpha'$ ) reactions is determined by a collective excitation of the aligned nucleus in the coupled-channel method, but that, in the former reaction, tensor forces should be taken into account in the potential of  $d^{24}\text{Mg}$  interaction.

The analogous analysis performed in the present study for the reaction  $^{24}\text{Mg}(p, p_1)^{24}\text{Mg}(2^+, 1.369 \text{ MeV})$  at  $E_p = 7.4 \text{ MeV}$  revealed that, in order

to describe correctly the resulting experimental correlation features, it is necessary to include the excitation of the  $3/2^+$  individual resonance in a  $^{25}\text{Al}$  compound nucleus in addition to taking into account the collective excitation mechanism within the coupled-channel method. The cross sections for elastic and inelastic proton scattering are differently sensitive to these mechanisms. As for the elastic-scattering cross section, it is determined almost exclusively by the collective-excitation mechanism within the rotational version of the coupled-channel method. At the same time, the inelastic-scattering cross section receives a significant contribution from the  $3/2^+$  resonance in the  $^{25}\text{Al}$  compound nucleus. Our calculations reproduced qualitatively the experimental angular dependences of the populations  $P_{\pm M}(\theta_p)$ , multipole-moment orientation tensors  $t_{k\kappa}(\theta_p)$ , and polarization tensors  $T_{k\kappa}(\theta_p)$ .

Several experimental orientation features of  $^{24}\text{Mg}$  nuclei formed in the  $2^+$  state at 1.369 MeV in inelastic proton, deuteron, and alpha-particle scattering on  $^{24}\text{Mg}$  at an energy of  $E_x \approx 7.5 \text{ MeV}$  per nucleon were found to be in general similar.

## REFERENCES

1. N. S. Zelenskaya and I. B. Teplov, *Properties of Excited States of Nuclei and Angular Correlations in Nuclear Reactions* (Energoatomizdat, Moscow, 1995) [in Russian].
2. L. I. Galanina, N. S. Zelenskaya, I. A. Konyukhova, V. M. Lebedev, N. V. Orlova, and A. V. Spassky, *Phys. At. Nucl.* **76**, 1415 (2013).
3. L. I. Galanina, N. S. Zelenskaya, I. A. Konyukhova, V. M. Lebedev, N. V. Orlova, A. V. Spassky, and S. V. Artemov, *Phys. At. Nucl.* **77**, 1421 (2014).
4. L. I. Galanina, N. S. Zelenskaya, I. A. Konyukhova, V. M. Lebedev, N. V. Orlova, A. V. Spassky, and S. V. Artemov, *Bull. Russ. Acad. Sci.: Phys.* **75**, 552 (2011).
5. L. I. Galanina, N. S. Zelenskaya, I. A. Konyukhova, V. M. Lebedev, N. V. Orlova, and A. V. Spassky, *Bull. Russ. Acad. Sci.: Phys.* **78**, 395 (2014).
6. K. Matsuda, Y. Nagahara, Y. Oda, et al., *Nucl. Phys.* **27**, 1 (1961).
7. L. I. Galanina, N. S. Zelenskaya, V. M. Lebedev, et al., *Bull. Russ. Acad. Sci. Phys.* **79**, 556 (2015).
8. T. Tamura, *Rev. Mod. Phys.* **37**, 679 (1965).
9. P. D. Kunz and E. Rost, *Comp. Nucl. Phys.* **2**, 88 (1993).
10. <http://www.fresco.org.uk/>
11. N. S. Zelenskaya, V. M. Lebedev, and A. V. Spassky, *Naukoemk. Tekhnol.* **4** (1), 19 (2003).

12. L. I. Galanina, N. S. Zelenskaya, V. M. Lebedev, N. V. Orlova, and A. V. Spassky, *Bull. Russ. Acad. Sci. Phys.* **76**, 422 (2012).
13. L. I. Galanina, N. S. Zelenskaya, V. M. Lebedev, N. V. Orlova, and A. V. Spassky, *Phys. At. Nucl.* **75**, 1331 (2012).
14. L. I. Galanina and N. S. Zelenskaya, *Phys. At. Nucl.* **63**, 1792 (2000).
15. <http://cdfc.sinp.msu.ru>
16. V. V. Lazarev, O. V. Chubinskii, R. P. Kolalis, et al., *Bull. Russ. Acad. Sci.: Phys.* **63**, 116 (1999).
17. L. I. Galanina and N. S. Zelenskaya, Preprint NIIYad. Fiz. MGU-99-21/579 (Moscow, 1999).
18. V. G. Neudatchin and Yu. F. Smirnov, *Nucleon Clusters in Light Nuclei* (Nauka, Moscow, 1969) [in Russian].
19. A. G. Sitenko, *Theory of Nuclear Reactions* (Energoatomizdat, Moscow, 1983), [in Russian].
20. A. J. Koning and J. P. Delaroche, *Nucl. Phys. A* **713**, 231 (2003).
21. L. I. Galanina, N. S. Zelenskaya, I. A. Konyukhova, et al., in *Igor Borisovich Teplov: On the Occasion of the 80th Birthday* (Universitetskaya Kniga, Moscow, 2008), p. 93 [in Russian].